

Performance Guarantees for Spectral Initialization in Rotation Averaging and Pose-Graph SLAM

Kevin J. Doherty^{*1}, David M. Rosen², and John J. Leonard¹

¹*Computer Science and Artificial Intelligence Laboratory, Massachusetts Institute of Technology, Cambridge, MA 02139, USA*

²*Laboratory for Information and Decision Systems, Massachusetts Institute of Technology, Cambridge, MA 02139, USA*

Abstract

In this work, we describe an initialization method based on *spectral relaxation* for rotation averaging and pose-graph optimization in the setting of simultaneous localization and mapping (SLAM). These optimization problems are typically both large-scale and nonconvex; in consequence, efficient methods for computing high-quality initial estimates are needed to enhance the speed and performance of the algorithms underlying these robot perception problems. To this end, we present an easily-implemented initialization method based on spectral relaxation tailored to the rotation averaging and SLAM problems. Critically, we also present error bounds controlling both the error of this estimate with respect to the ground truth as well as its distance to the corresponding *global minimizer* of the problem. These are, to our knowledge, *the first such performance guarantees for spectral initializations to rotation averaging and pose-graph SLAM*. The form of our bounds reveals the spectral properties of the measurement graphs to be central objects of interest in controlling these quantities. Moreover, our analysis is based upon new error bounds for global minimizers, which are likely to be of independent interest. Finally, our empirical results suggest that spectral estimates typically perform far better than the worst-case analysis suggests, producing comparable or higher-quality initializations to state-of-the-art techniques with lower computational cost.

1 Introduction

Simultaneous localization and mapping (SLAM), the process by which a robot jointly infers its pose and the location of environmental landmarks, is a fundamental capability of mobile robots, supporting navigation, planning, and control [25]. State-of-the-art SLAM methods typically rely on nonconvex optimization. This nonconvexity is due to the constraint that robot rotation estimates lie in the special orthogonal group $\text{SO}(d)$, which is a nonconvex set. In consequence, the quality of a recovered SLAM estimate crucially depends upon the quality of the initial guess, and a great deal of research has been dedicated to initialization techniques (see Carlone et al. [9] for a review). While these techniques have been shown to work well in practice, the reasons for their empirical success are currently poorly understood. As a result, it is difficult to say when, or under what conditions, these techniques can be reliably deployed.

^{*}Corresponding author. Email: kjd@csail.mit.edu

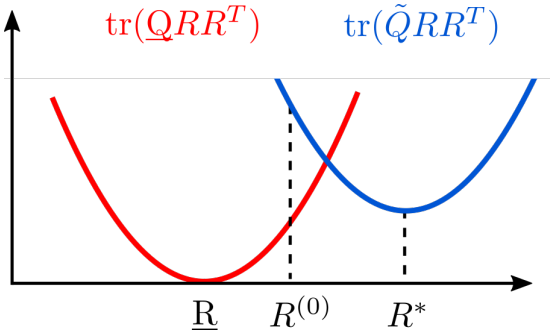


Figure 1: **Comparing true, optimal, and initial rotation estimates.** We are interested in bounds on the deviation of an initial estimate $R^{(0)}$ from the (latent) ground truth \underline{R} and the globally optimal solution R^* .

This work provides *the first guarantees* on the error of an initialization method its deviation from the globally optimal solution, for the fundamental problems of pose-graph SLAM and rotation averaging. Our analysis gives direct control over the error of a *spectral initialization* in terms of the spectral properties of the measurement graph¹. This allows us to control the distance of the spectral estimate to the corresponding global minimizer, which is critical for ensuring that the initial guess is in the correct basin of attraction, and therefore that the global minimizer can be recovered by local search (see Figure 1). Our proof of this result relies on new estimation error bounds for global optima, which are likely to be of independent interest. Moreover, the approach is easily implemented using any off-the-shelf eigensolver (e.g. MATLAB `eigs`). Our empirical results on both synthetic data and standard pose-graph SLAM benchmarks demonstrate that the spectral estimator typically performs far better than our worst-case analysis suggests, achieving solution quality and computation times competitive with state-of-the-art approaches. Beyond the immediate interpretation of these results as an analysis of an *initialization method* for optimization, our results reveal the spectral relaxation to be an inexpensive method for computing rotation averaging and pose-graph optimization solutions on its own (without the need to perform nonconvex optimization or semidefinite relaxation) that attains similar worst-case performance guarantees to the global optimum.

The remainder of the paper proceeds as follows: In Section 2, we discuss related literature on robot perception and rotation synchronization. In Section 3 we describe the problem formulation, and Section 4 describes the spectral initialization procedure. In Section 5 we present our main results: an analysis controlling the estimation error of both the spectral initialization method and that of globally optimal estimates for the rotation averaging and pose-graph SLAM problems, as well as a bound on the distance between the spectral initialization and the globally optimal solution. Section 6 demonstrates the empirical performance of the spectral initialization technique on benchmark SLAM datasets, together with our performance bound evaluated on synthetic data and shows, in particular, that the spectral estimator is competitive with state-of-the-art techniques for initialization.

¹Recent work has identified spectral properties of measurement graphs as key quantities controlling the performance of estimators for these problems, though this connection (particularly in the context of SLAM) remains under-explored (see [25] for a recent review).

2 Related work

Simultaneous localization and mapping and rotation averaging problems are often formulated as high-dimensional, nonconvex optimization problems. Consequently, solving these problems typically requires efficient algorithms for producing an “initial guess.” Historically, research on this topic has focused on developing cheap, but typically inexact, convex or linear relaxations of the SLAM (resp. rotation averaging) problems (cf. [9, 20]). While these techniques often work well in practice, the *reasons* for their empirical success remain poorly understood, and it is difficult to assess *under which conditions* these techniques can be reliably deployed.

A related line of research is the development of Cramér-Rao bounds, which provide lower bounds on the expected error of unbiased estimators for these problems. Our analysis complements previous work in this area by Boumal et al. [6], Khosoussi et al. [17], and Chen et al. [11]. Such bounds control the *best* possible error of an estimator *in expectation*. In contrast, the bounds we present control the *worst-case* error on a *per instance* basis. Interestingly, our analysis, consistent with prior work, reveals the spectral properties of the graph parameterizing the estimation problem to be central objects of interest in controlling the estimation error (cf. [6, 11, 17]).

The spectral relaxation approach to initialization that we consider has previously appeared in other problem settings, particularly in the area of phase synchronization problems (cf. [4, 5, 18, 26]). In particular, Ling [18] describe error bounds that are qualitatively similar to those described in this paper, though theirs are concerned specifically with *orthogonal* group synchronization problems. Liu et al. [19] take a similar approach to ours in order to derive error bounds for spectral estimators of synchronization problems defined over subgroups of the orthogonal group (including $\text{SO}(d)$), though the form of the bounds we develop makes the connection between estimation error and the spectral properties of the measurement graphs more explicit.

Recently, Moreira et al. [21] proposed a computationally-efficient Krylov-Schur decomposition approach for pose-graph SLAM. One can show that their method is formally equivalent to the *rotation-only* variant of the spectral initialization procedure considered here, but our construction arises more directly and simply from convex relaxation. Arrigoni et al. [1] describe a spectral method for $\text{SE}(d)$ -synchronization. An analysis similar to ours can be carried out for theirs as well, but the form of the relaxation they consider leads to more complicated bounds due to a dependence on the absolute translation scale. Finally, Boots and Gordon [3] consider spectral techniques for the range-only problem. Though their problem setting differs from the one considered here, extension of the techniques presented in this work to scenarios with different types of measurement models is an interesting area for future work.

Recently, *certifiably-correct* machine perception has emerged as a key area of interest to the robotics community, resulting in the development of algorithms capable of recovering globally optimal solutions in certain noise regimes [7, 8, 10, 12, 13, 24, 28]. Our analysis gives direct control over the estimation error for these solutions in terms of the magnitude of the measurement noise. Moreover, the bounds we present suggest that these estimators, which are often based on large-scale semidefinite relaxations, admit similar *worst-case* performance guarantees to an estimate computed using the proposed spectral method. While it may be difficult to compute (or impossible to verify) a solution using the former methods, the spectral estimator is always available, and as we show, can typically be computed inexpensively.

3 Preliminaries and formulation

3.1 Notation and preliminaries

Lie groups: We will make use of the matrix realizations of several Lie groups, most prominently the d -dimensional special Euclidean and special orthogonal groups, denoted $\text{SE}(d)$ and $\text{SO}(d)$, respectively. The realization of $\text{SE}(d)$ as a matrix group can be defined as follows:

$$\text{SE}(d) \triangleq \left\{ \begin{bmatrix} R & t \\ 0 & 1 \end{bmatrix} \in \mathbb{R}^{(d+1) \times (d+1)} \mid R \in \text{SO}(d), t \in \mathbb{R}^d \right\}, \quad (1)$$

and the group $\text{SO}(d)$ can be realized as:

$$\text{SO}(d) \triangleq \left\{ R \in \mathbb{R}^{d \times d} \mid R^T R = I_d, \det(R) = 1 \right\}. \quad (2)$$

Linear algebra: For a symmetric matrix S , $S \succeq 0$ denotes that S is positive-semidefinite. The eigenvalues of a symmetric matrix $S \in \mathbb{R}^{n \times n}$ are denoted $\lambda_1(S) \leq \lambda_2(S) \leq \dots \leq \lambda_n(S)$. We will also consider several block-structured matrices and make use of a few special operators acting on block-structured matrices. Following the notation of Rosen et al. [24], given square matrices $A_i \in \mathbb{R}^{d \times d}$, $i = 1, \dots, n$, we let $\text{Diag}(A_1, \dots, A_n)$ denote the matrix with each A_i along the diagonal (i.e. the matrix direct sum). Furthermore, given a block-structured matrix B , let $\text{BlockDiag}_d(B)$ denote the operator extracting the $d \times d$ block-diagonal entries of B . Finally, let $\text{SBD}(d, n)$ denote the set of $dn \times dn$ symmetric block-diagonal matrices with diagonal blocks of size $d \times d$, and $\text{SymBlockDiag}_d(A)$ be the operator extracting the symmetric part of the $d \times d$ block-diagonal elements of A .

Probability and statistics: We denote the multivariate Gaussian distribution with mean $\mu \in \mathbb{R}^d$ and covariance $\Sigma \in \mathbb{S}^d$ as $\mathcal{N}(\mu, \Sigma)$. We denote the isotropic Langevin distribution on $\text{SO}(d)$ with mode $M \in \text{SO}(d)$ and concentration parameter $\kappa \geq 0$ as $\text{Langevin}(M, \kappa)$. The probability density function for the isotropic Langevin distribution is given as:

$$p(R; M, \kappa) = \frac{1}{c_d(\kappa)} \exp(\kappa \text{tr}(M^T R)), \quad (3)$$

where $c_d(\kappa)$ is a normalization constant.

Finally, for an unknown variable Z we aim to infer, we denote its true latent value by Z and \tilde{Z} denote a noisy measurement of Z .

Gauge-invariant distance metrics: A key property of the problems under consideration is *gauge symmetry*. Synchronization problems over $\text{SO}(d)$ and $\text{SE}(d)$ with $d \geq 2$ admit infinitely many solutions. In particular, we will see that if $R^* \in \text{SO}(d)^n$ is an optimal estimate of the rotational states, then GR^* is also optimal for any $G \in \text{SO}(d)$. We therefore define the following *orbit distances* in order to compare solutions to the problems at hand:

$$d_{\mathcal{S}}(X, Y) \triangleq \min_{G \in \text{SO}(d)} \|X - GY\|_F, \quad X, Y \in \text{SO}(d)^n \quad (4a)$$

$$d_{\mathcal{O}}(X, Y) \triangleq \min_{G \in \text{O}(d)} \|X - GY\|_F, \quad X, Y \in \text{O}(d)^n. \quad (4b)$$

It will be convenient to “overload” the $\text{O}(d)$ orbit distance to act on elements of the Stiefel manifold $\text{St}(dn, d)$. That is, for $X, Y \in \text{St}(dn, d)$:

$$d_{\mathcal{O}}(X, Y) \triangleq \min_{G \in \text{O}(d)} \|X - GY\|_F. \quad (5)$$

Each of these distances can be computed in closed form (cf. Rosen et al. [24]).

3.2 Problem formulation

We consider the problem of synchronization over the $\text{SO}(d)$ group: this is the problem of estimating n unknown values $R_1, \dots, R_n \in \text{SO}(d)$ given a set of noisy measurements \tilde{R}_{ij} of a subset of their pairwise relative rotations. The problem of $\text{SO}(d)$ -synchronization captures, in particular, the problems of rotation averaging and, under common modeling assumptions, pose graph optimization, where the variables of interest are the orientations of a robot (or more generally, a rigid body) at different points in time (see, for example Grisetti et al. [14]). This problem possesses a natural graphical structure $\mathcal{G} \triangleq (\mathcal{V}, \vec{\mathcal{E}})$, where nodes \mathcal{V} correspond to latent variables $R_i \in \text{SO}(d)$ and edges $(i, j) \in \vec{\mathcal{E}}$ correspond to (noisy) measured relative rotations \tilde{R}_{ij} between R_i and R_j . In particular, for the problem of *rotation averaging*, we adopt the following standard generative model for rotation measurements: For each edge $(i, j) \in \vec{\mathcal{E}}$ (cf. [12, 24]):

$$\tilde{R}_{ij} = \underline{R}_{ij} R_{ij}^\epsilon, \quad R_{ij}^\epsilon \sim \text{Langevin}(I_d, \kappa_{ij}), \quad (6)$$

where I_d is the $(d \times d)$ identity matrix. Given a set of noisy pairwise relative rotations \tilde{R}_{ij} sampled according to the generative model (6), a maximum-likelihood estimate $R^* \in \text{SO}(d)^n$ for the latent rotational states R_1, \dots, R_n is obtained as a minimizer of the following problem (cf. [12, 24]):

Problem 1 (Maximum-likelihood estimation for rotation averaging).

$$\min_{R_i \in \text{SO}(d)} \sum_{(i, j) \in \vec{\mathcal{E}}} \kappa_{ij} \|R_j - R_i \tilde{R}_{ij}\|_F^2. \quad (7)$$

For pose-graph SLAM ($\text{SE}(d)$ -synchronization), we adopt the following generative model for rotation and translation measurements: For each edge $(i, j) \in \vec{\mathcal{E}}$:

$$\tilde{R}_{ij} = \underline{R}_{ij} R_{ij}^\epsilon, \quad R_{ij}^\epsilon \sim \text{Langevin}(I_d, \kappa_{ij}) \quad (8a)$$

$$\tilde{t}_{ij} = \underline{t}_{ij} + t_{ij}^\epsilon, \quad t_{ij}^\epsilon \sim \mathcal{N}(0, \tau_{ij}^{-1} I_d), \quad (8b)$$

where $x_{ij} = (t_{ij}, R_{ij})$ is the true value of x_{ij} . That is, $x_{ij} = \underline{x}_i^{-1} \underline{x}_j$ given the true values of poses x_i and x_j . Under this noise model, the typical nonlinear least-squares formulation of $\text{SE}(d)$ synchronization is written as follows:

Problem 2 (Maximum-likelihood estimation for $\text{SE}(d)$ synchronization).

$$\min_{\substack{t_i \in \mathbb{R}^d \\ R_i \in \text{SO}(d)}} \sum_{(i, j) \in \vec{\mathcal{E}}} \kappa_{ij} \|R_j - R_i \tilde{R}_{ij}\|_F^2 + \tau_{ij} \|t_j - t_i - R_i \tilde{t}_{ij}\|_2^2. \quad (9)$$

Under these modeling assumptions, both pose-graph optimization and rotation averaging can be written in the following form:

Problem 3 (Rotation averaging and pose-graph optimization (Rotation synchronization form)).

$$p^* = \min_{R \in \text{SO}(d)^n} \text{tr}(\tilde{Q} R^\top R), \quad (10)$$

where $\tilde{Q} \in \text{Sym}(dn)$, $\tilde{Q} \succeq 0$. In particular, we have:

$$\tilde{Q} = L(\tilde{G}^\rho) \quad (\text{RA})$$

$$\tilde{Q} = L(\tilde{G}^\rho) + \underbrace{\tilde{\Sigma} - \tilde{V}^T L(W^\tau)^\dagger \tilde{V}}_{\tilde{Q}^\tau}. \quad (\text{PGO})$$

For our purposes, the specific structure of \tilde{Q} is not important. We only require that in the *noiseless* case where $\tilde{Q} = Q$, we have that $\underline{R}^T \in \ker(Q)$ where \underline{R} is the latent ground-truth assignment to the rotation estimates. Nonetheless, the complete definition of \tilde{Q} follows.

Here $L(W^\tau)$ denotes the Laplacian of the translation weight graph $W^\tau \triangleq (\mathcal{V}, \mathcal{E}, \{\tau_{ij}\})$ with *undirected edges* $\{i, j\} \in \mathcal{E}$, which is an $n \times n$ matrix with i, j -entry:

$$L(W^\tau)_{ij} = \begin{cases} \sum_{e \in \delta(i)} \tau_e, & i = j, \\ -\tau_{ij}, & \{i, j\} \in \mathcal{E}, \\ 0, & \{i, j\} \notin \mathcal{E} \end{cases} \quad (12)$$

Similarly, $L(\tilde{G}^\rho)$ denotes the *connection Laplacian* for the rotational measurements, which is a $dn \times dn$ symmetric block-diagonal matrix with $d \times d$ blocks determined by:

$$L(\tilde{G}^\rho)_{ij} \triangleq \begin{cases} d_i^\rho I_d, & i = j, \\ -\kappa_{ij} \tilde{R}_{ij}, & \{i, j\} \in \mathcal{E}, \\ 0_{d \times d}, & \{i, j\} \notin \mathcal{E}, \end{cases} \quad (13a)$$

$$d_i^\rho \triangleq \sum_{e \in \delta(i)} \kappa_e, \quad (13b)$$

where $\delta(i)$ denotes the set of edges *incident to* node i . $\tilde{V} \in \mathbb{R}^{n \times dn}$ denotes the $(1 \times d)$ -block-structured matrix with (i, j) block given by:

$$\tilde{V}_{ij} \triangleq \begin{cases} \sum_{e \in \delta^-(j)} \tau_e \tilde{t}_e^T, & i = j, \\ -\tau_{ji} \tilde{t}_{ji}^T, & (j, i) \in \vec{\mathcal{E}}, \\ 0_{1 \times d}, & \text{otherwise.} \end{cases} \quad (14)$$

Finally, let $\tilde{\Sigma} \in \text{SBD}(d, n)$ denote the symmetric block-structured diagonal matrix given by:

$$\begin{aligned} \tilde{\Sigma} &\triangleq \text{Diag}(\tilde{\Sigma}_1, \dots, \tilde{\Sigma}_n) \in \text{SBD}(d, n) \\ \tilde{\Sigma}_i &\triangleq \sum_{e \in \delta^-(i)} \tau_e \tilde{t}_e \tilde{t}_e^T, \end{aligned} \quad (15)$$

where $\delta^-(i)$ denotes the set of edges *leaving* node i .

4 Spectral methods for initialization

The nonconvexity of the $\text{SO}(d)$ constraint renders Problem 3 computationally hard to solve in general. Spectral methods for synchronization simplify the problem by relaxing the $\text{SO}(d)$ constraint to the constraint $YY^T = nI_d, Y \in \mathbb{R}^{d \times dn}$:

Problem 4 (Spectral Relaxation of the Rotation Synchronization Problem).

$$\begin{aligned} p_S^* &= \min_{Y \in \mathbb{R}^{d \times dn}} \text{tr}(\tilde{Q} Y^T Y) \\ \text{s.t. } &YY^T = nI_d. \end{aligned} \quad (16)$$

Algorithm 1 Spectral Initialization procedure

Input: The data matrix \tilde{Q} from (RA) or (PGO)
Output: A spectral initialization $R^{(0)}$

```

1: function SPECTRALINITIALIZATION( $\tilde{Q}$ )
2:   Compute the  $d$  eigenvectors  $\Phi$  of  $\tilde{Q}$  with smallest eigenvalues      ▷ Solve Problem 4.
3:   for  $i = 1, \dots, n$  do
4:     Set  $R_i^{(0)} \leftarrow \Pi_S(\Phi_i)$ , where  $\Phi_i$  is the  $i$ -th ( $d \times d$ ) block of  $\Phi$ .    ▷ Definition 1
5:   end for
6:   return  $R^{(0)}$ 
7: end function

```

These methods are termed *spectral* relaxations due to their connection to the eigenvectors of the data matrix \tilde{Q} . In particular, it is straightforward to verify that an estimate Y^* is a minimizer for Problem 3 if and only if Y^* consists of the d eigenvectors corresponding to the minimum d eigenvalues of \tilde{Q} .

For the noiseless problem parameterized by Q , the relaxation in Problem 4 is exact in the sense that $R = Y^*$. This follows from the fact that by construction, the ground truth rotations R^\top lie in $\ker(Q)$,² and $RR^\top = nI_d$ since $R \in \text{SO}(d)^n$. In general, however, we do not expect such a straightforward relationship between a minimizer of the spectral relaxation in Problem 4 and a corresponding minimizer of Problem 3. In such cases where exactness does not hold, we can *round* the estimate provided by the spectral relaxation to an approximate solution $R^{(0)} \in \text{SO}(d)^n$ in the feasible set of Problem 3. The following definition makes this precise.

Definition 1 (Projection onto $\text{SO}(d)$). Let $X \in \mathbb{R}^{d \times d}$, the projection $\Pi_S(X)$ of X onto $\text{SO}(d)$ is by definition a minimizer of the following:

$$\Pi_S(X) \triangleq \underset{G \in \text{SO}(d)}{\operatorname{argmin}} \|X - G\|_F. \quad (17)$$

A minimizer for this problem is given in closed-form as (cf. [15, 29]):

$$\Pi_S(X) = U\Sigma V^\top. \quad (18)$$

where $U\Sigma V^\top$ is a singular value decomposition of X , and Σ is the matrix:

$$\Sigma = \text{Diag}(1, 1, \det(UV^\top)) \quad (19)$$

In the context of subsequent derivations, it will be convenient to “overload” this rounding operation to $Y \in \mathbb{R}^{d \times dn}$ as follows:

$$\Pi_S(Y) = (\Pi_S(Y_1), \dots, \Pi_S(Y_n)), \quad (20)$$

where $Y_i \in \mathbb{R}^{d \times d}$ are the n blocks of Y .

Therefore, we can obtain an approximate solution to Problem 3 from a minimizer Y^* of the relaxation in Problem 4 as $R^{(0)} \triangleq \Pi_S(Y^*)$. This entire procedure is summarized in Algorithm 1.

5 Main results

This section presents our main results, which are three-fold: First, we provide a bound on the error of a spectral initialization $R^{(0)}$ with respect to the ground-truth rotations R . Second, we

²We refer the reader to [24, Appendix C.3] for detailed analysis of the noiseless case.

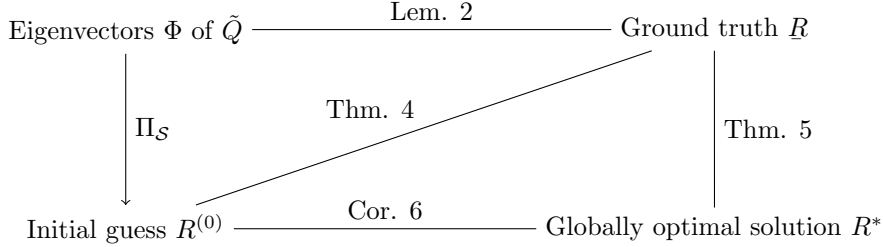


Figure 2: **Guide to the theoretical bounds.** This figure presents a diagrammatic guide to the bounds presented in Section 5. In particular, Lemma 2 gives a bound on the orbit distance between the eigenvectors of the data matrix and the ground truth. We then use this result in Theorem 4, giving a bound on the deviation of the spectral initialization from the ground truth. In Theorem 5 we bound the deviation of a *globally optimal solution* to the maximum likelihood estimation problems for rotation averaging and pose-graph SLAM from the ground truth. Finally, relating these bounds we obtain Corollary 6, which bounds the distance between a spectral initialization and the globally optimal solution.

give a new bound on the error of *globally optimal* solutions R^* with respect to R : this bound differs from prior work (e.g. Preskitt [22], Rosen et al. [24]) in that it is defined with respect to the orbit distance on $\text{SO}(d)^n$. Previous work used the orbit distance on $\text{O}(d)^n$ due to mathematical convenience; however, the estimation error one considers in application is over $\text{SO}(d)^n$, since this is the domain on which the estimation problem is defined. Combining these results, we obtain an upper bound on the $\text{SO}(d)$ orbit distance between an initial guess $R^{(0)}$ and a globally optimal solution R^* . Our analysis gives direct control over the mutual deviation between the three quantities of interest: $R^{(0)}$, R^* , and R as a function of the noise magnitude. We conclude with additional remarks about computing these bounds for practical SLAM scenarios and a few straightforward adaptations of the main results. Figure 2 gives an overview of the main results.

Recall from Problem 4 that an estimate Φ is a minimizer of Problem 4 if and only if it is comprised of a set of the minimum d eigenvectors³ of \tilde{Q} , and that in the noiseless case this minimizer is given by R . Since a spectral initialization $R^{(0)}$ is obtained as the projection of the solution Φ of Problem 4 onto $\text{SO}(d)^n$, we can bound its estimation error by first bounding the deviation of Φ from R , then bounding the additional error incurred by projecting onto $\text{SO}(d)^n$.

We can bound the deviation of a solution Φ of Problem 4 from the ground truth R via the Davis-Kahan Theorem [30], a classical result relating the perturbation of a matrix’s eigenvectors under a symmetric perturbation to the magnitude of that perturbation. Here, we take Q to be the matrix under consideration, and define the perturbation $\Delta Q \triangleq \tilde{Q} - Q$. The following lemma gives the desired characterization:

Lemma 2. *Let Φ be a minimizer of Problem 4 and R be the corresponding ground truth rotations. Then:*

$$d_{\mathcal{O}}(R, \Phi) \leq \frac{2\sqrt{2dn}\|\Delta Q\|_2}{\lambda_{d+1}(Q)}. \quad (21)$$

Lemma 2 provides control over the deviation of an “unrounded” solution Φ from the ground truth. The second technical ingredient we require is the following simple bound controlling the maximum distance between a matrix X and its projection $\Pi_S(X)$ onto $\text{SO}(d)$:

Lemma 3. *Let $X \in \mathbb{R}^{d \times d}$ and $R \in \text{SO}(d)$. Then:*

$$\|\Pi_S(X) - R\|_F \leq 2\|X - R\|_F. \quad (22)$$

³By “minimum d eigenvectors” we mean the eigenvectors corresponding to the minimum d eigenvalues.

Proof.

$$\|\Pi_S(X) - R\|_F = \|\Pi_S(X) - X + X - R\|_F \quad (23)$$

$$\leq \|\Pi_S(X) - X\|_F + \|X - R\|_F \quad (24)$$

$$\leq 2\|X - R\|_F, \quad (25)$$

where the last inequality follows from the fact that $\Pi_S(X)$ is a minimizer over $\text{SO}(d)$ of the distance to X with respect to the Frobenius norm, and that, by hypothesis, $R \in \text{SO}(d)$. \square

Lemma 3 provides a straightforward approach for converting a bound expressed in the $\text{O}(d)^n$ orbit distance to one expressed in the $\text{SO}(d)^n$ orbit distance. In turn, we obtain the following theorem:

Theorem 4. *Let Φ be a minimizer of Problem 4 and $R^{(0)} = \Pi_S(\Phi) \in \text{SO}(d)^n$ be the corresponding spectral initialization. Finally, let $R \in \text{SO}(d)^n$ be set of ground truth rotations in Problem 3. Then the estimation error of $R^{(0)}$ satisfies:*

$$d_S(\underline{R}, R^{(0)}) \leq \frac{4\sqrt{2dn}\|\Delta Q\|_2}{\lambda_{d+1}(\underline{Q})}. \quad (26)$$

The bound (26) gives a direct (linear) relationship between the magnitude of the perturbation ΔQ and the worst-case error of a spectral estimate. Moreover, Theorem 4 implies that $d_S(\underline{R}, R^{(0)}) \rightarrow 0$ as $\Delta Q \rightarrow 0$. That is to say, as the measurements approach their noiseless counterparts, we recover the ground truth.

Next, we address the issue of furnishing a bound on $d_S(\underline{R}, R^*)$. The following theorem gives the desired bound:

Theorem 5 (Bounding the estimation error for R^*). *Let R^* be a minimizer of Problem 3 and R be the set of ground-truth rotations. Then the estimation error of R^* satisfies:*

$$d_S(\underline{R}, R^*) \leq \frac{8\sqrt{dn}\|\Delta Q\|_2}{\lambda_{d+1}(\underline{Q})}. \quad (27)$$

We are not aware of any prior bounds that control the estimation error of a maximum-likelihood estimate R^* over $\text{SO}(d)^n$ specifically. Prior work considered the estimation error over $\text{O}(d)^n$ [2, 18, 24]. In our application, however, we are specifically concerned with the estimation error over $\text{SO}(d)^n$; as one can see from inspection, this is the domain on which Problem 3 is defined. Thus, the $\text{SO}(d)^n$ orbit distance corresponds to the *actual* error one would obtain in practice.

While Theorem 4 establishes error bounds for the spectral estimator, when viewed as an *initialization method*, the distance between the initial guess $R^{(0)}$ and the globally optimal solution is the primary concern. A corollary to Theorems 4 and 5, allows us to control $d_S(R^{(0)}, R^*)$ in terms of the noise matrix ΔQ . We have:

Corollary 6. *The distance between the initialization $R^{(0)}$ and the globally optimal solution R^* satisfies:*

$$d_S(R^{(0)}, R^*) \leq \frac{(8 + 4\sqrt{2})\sqrt{dn}\|\Delta Q\|_2}{\lambda_{d+1}(\underline{Q})}. \quad (28)$$

These bounds provide a clear relationship between the spectral properties of \underline{Q} and ΔQ and the deviation between a spectral estimator $R^{(0)}$, maximum-likelihood estimator R^* , and the ground-truth \underline{R} . An important consequence of these bounds is that as $\Delta Q \rightarrow 0$, we have (at

least) linear convergence of the estimation error for *both* the spectral estimator and the maximum-likelihood estimator to zero. This, in turn, guarantees that $\Delta Q \rightarrow 0$ implies $R^*, R^{(0)} \rightarrow R$ (up to symmetry), which is what we would expect.

In practice, however, we do not have access to Q . This presents some difficulty in the computation of ΔQ and $\lambda_{d+1}(Q)$. Fortunately, the noiseless rotation matrices admit a description in terms of quantities that *are* typically assumed to be known. In particular, we have (cf. [24, Lemma 8]):

$$\lambda_{d+1}(L(G^\rho)) = \lambda_2(L(W^\rho)), \quad (29)$$

where $L(W^\rho)$ is the Laplacian of the rotation weight graph. Now, $L(W^\rho)$ depends only on the concentration parameters κ_{ij} attached to each edge, which are generally assumed to be known *a priori* from the noise models (6) and (8). In the rotation averaging case, we have $Q = L(G^\rho)$, and therefore the denominator $\lambda_{d+1}(Q)$ is readily available as $\lambda_2(L(W^\rho))$, the algebraic connectivity of the rotational weight Laplacian.

In the case of pose-graph SLAM, where the matrix Q contains the translational terms Q^τ , we can use the fact that $Q = L(G^\rho) + Q^\tau$ is the sum of positive-semidefinite matrices, so $\lambda_{d+1}(L(G^\rho)) \leq \lambda_{d+1}(L(G^\rho) + Q^\tau) = \lambda_{d+1}(Q)$. In particular, the (weaker) bounds obtained by substituting $\lambda_{d+1}(Q)$ with $\lambda_{d+1}(L(G^\rho))$ in (26) and (27) hold.

Moreover, a common SLAM initialization technique is that of *rotation only initialization* – i.e., to compute the initializer $R^{(0)}$ using *only* the relative rotation measurements [9]. This can have computational advantages in practice since $L(\tilde{G}^\rho)$ is generally *sparse*; the same cannot be said for the pose-graph SLAM data matrix \tilde{Q} , as it arises via analytic elimination of the translational states, in which the resulting data matrix \tilde{Q} is formed as a (dense) generalized Schur complement (cf. [24]). Interestingly, for pose-graph SLAM, a spectral initialization $R^{(0)}$ computed using the eigenvectors of $L(\tilde{G}^\rho)$ (i.e. ignoring \tilde{Q}^τ) attains the bound:

$$d_S(R, R^{(0)}) \leq \frac{4\sqrt{2dn}\|\Delta L(\tilde{G}^\rho)\|_2}{\lambda_{d+1}(L(G^\rho))}. \quad (30)$$

This bound holds by the same reasoning as Theorem 4, but with the consideration that $R^T \in \ker(L(G^\rho))$.

As a final consideration, typically we also do not have access to ΔQ . If we had access to ΔQ , we could recover the true data matrix Q as $\tilde{Q} - \Delta Q$. In consequence, we need a method to estimate the likely magnitude of the noise in a given application. One way of achieving this is via simulation from the generative model, given a measurement network and associated measurement precisions.⁴ This, in turn, gives a *distribution* over the bounds (26), (27), and (28).

6 Experimental results

In this section, we compare the bounds in Theorem 4 to the actual estimation error of the spectral initialization and globally optimal pose-graph SLAM solutions. In Section 6.1 we construct synthetic pose-graph SLAM scenarios for which the ground-truth poses are known. Since the bounds we have presented depend upon knowledge of the noise magnitude $\|\Delta Q\|_2$ and the spectral gap of the *true* data matrix Q , which are unknown in practice for pose-graph SLAM, our first set of empirical results shed light on the behavior of these worst-case bounds (as well as the *actual* error realized by different estimators) as we vary the noise parameters controlling the generative model (8).

⁴Simulating measurements in the case of pose-graph SLAM requires knowledge of the ground-truth translation measurement scale, which is typically also unavailable in practice. However, the *rotation-only* initialization bound (30) applies in general and depends only upon the rotation measurements, which can be simulated to produce an empirical bound.

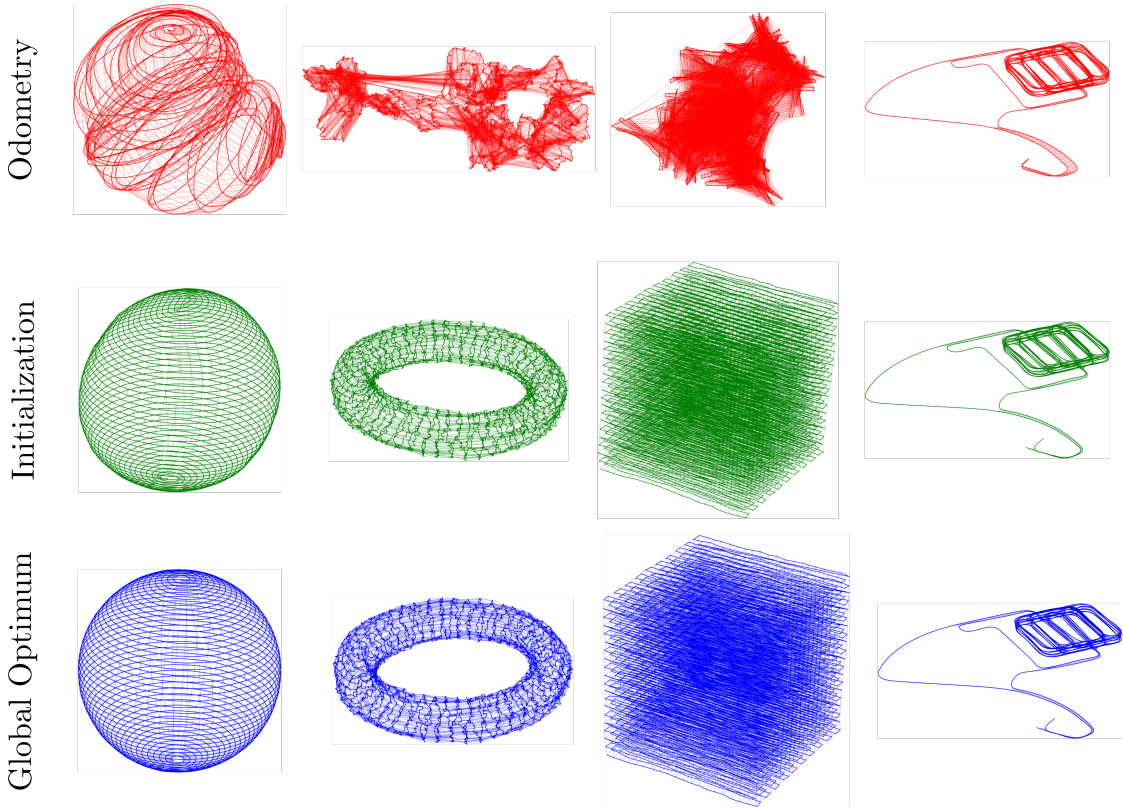


Figure 3: Spectral relaxation produces high-quality initializations. Qualitative comparison with the globally optimal solution suggests that the spectral relaxation produces estimates that are very close to the globally optimal solution for a variety of SLAM benchmark datasets.

In Section 6.2, we evaluate the performance of spectral relaxation as a practical initialization method in the context of 3D pose-graph SLAM applications. We show that, consistent with our results on synthetic data, the spectral initialization method offers high-quality initial solutions for pose-graph optimization, and, in particular, that the inclusion of translation data when computing a spectral estimator improves the objective value of the initial estimate compared to the common approach of using exclusively rotation data.

The spectral initialization method was implemented in C++ using Spectra to efficiently solve large-scale eigenvalue problems [23]. Computation of the bounds in Section 6.1 was performed in MATLAB using `eigs`. All experiments were performed on a laptop with a 2.2 GHz Intel i7 CPU. Where (verified) globally optimal solutions were needed, we used the C++ implementation of SE-Sync [24]. We also provide results using the well-known *chordal* initialization method [20], which relaxes the feasible set of Problem 3 to $\mathbb{R}^{d \times dn}$, with the constraint that $R_1^{(0)} = I_d$, for which the solution can be obtained by solving a linear system.

6.1 Evaluation on synthetic data

The bounds presented in our analysis depend upon knowledge of the noise magnitude $\|\Delta Q\|_2$, which is unknown in practice. In light of this fact, we examine empirically the behavior of the bounds as a function of the noise parameters using synthetic data. Specifically, we use the Cube dataset [8, 24], which consists of a set of vertices (poses) organized in a three-dimensional

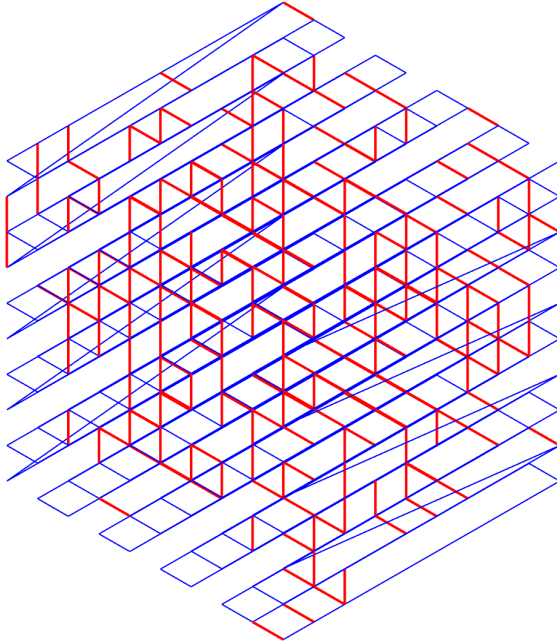


Figure 4: **Cube experiments.** Ground truth poses for the synthetic Cube dataset [8, 24] with $s = 10$ vertices per side and $p_{LC} = 0.1$. The robot’s trajectory is shown in blue with loop closures shown in red.

cube, with s vertices per dimension. Consecutive poses have an “odometry” edge between them, and loop closures are sampled randomly from the remaining edges with probability p_{LC} . Measurements are generated by randomly sampling from the generative model (8) with fixed noise parameters κ and τ for all measurements. Beyond providing access to the ground-truth rotations, this setup allows us to compare the worst-case bounds with empirical performance in noise regimes well outside the range typically encountered in real SLAM scenarios. A sample configuration for the Cube dataset is provided in Figure 4.

Influence of noise parameters on performance bounds: In Figure 5, we study the performance of the spectral initialization approach across a variety of typical noise configurations. In each case, we provide the worst-case bounds (26) and (30) along with the empirical error of the different estimators under consideration. In Figure 5a, we sample Cube problem instances with logarithmically spaced values of κ while fixing the other parameters: $\tau = 150$, $p_{LC} = 0.2$, and $s = 10$. In Fig. 5b, we fix $\kappa = 10^5$, $p_{LC} = 0.25$ and $s = 10$ and sample problem instances with logarithmically-spaced translation concentration parameter τ . In Fig. 5c, we fix $\kappa = 10^5$, $\tau = 150$, $s = 10$ and vary p_{LC} from 0 to 1.

Across a wide range of concentration parameters, the spectral initializations attain very similar error to the global optimizer.⁵ In particular, their error often improves upon the worst-case bounds (26) and (30) by orders of magnitude. This is consistent with earlier observations of qualitatively similar bounds for phase synchronization [22]. Moreover, in practical applications of rotation averaging and pose-graph optimization, previous work has shown that the maximum-likelihood estimator often attains expected error close to the Cramér-Rao *lower bound* (see [6]

⁵ R^* is the maximum-likelihood estimator—the optimal point estimate given the data. Since there is noise in the data, it is conceivable that the maximum-likelihood estimate might actually be farther away from the ground truth than a “suboptimal” estimate, which we observe in Fig. 5a.

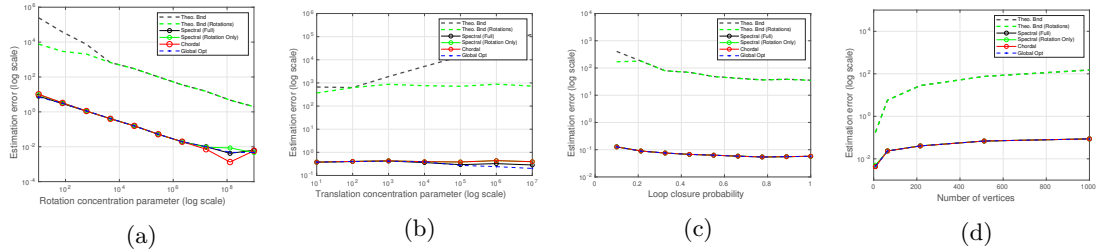


Figure 5: **Influence of dataset parameters on the performance bounds for the Cube experiments.** We examine empirically the change in the theoretical bounds (26) and (30) as well as the estimation error of several pose-graph optimization estimates while varying (a) the rotation concentration parameter κ , (b) the translation concentration parameter τ , (c) the probability of a loop closure p_{LC} , (d) the number of vertices s^3 .

for rotation averaging and [11] for pose-graph optimization). The specific case varying the translation concentration parameter in Figure 5b is interesting, since while the spectral estimator improves with increasing τ , the bound suggests the opposite worst-case behavior. This apparent mismatch warrants further investigation, and impacts prior bounds for pose-graph optimization, e.g. in [24]. With this exception, the bounds seem to accurately capture the behavior of the actual estimation error.

Dependence on problem dimensionality: Due to the explicit appearance of the problem dimension n in the bounds (26), (27), and (28), it is interesting to consider how the number of rotations to be estimated affects these bounds. In Figure 5d, we fix $\kappa = 10^5, \tau = 150, p_{LC} = 0.2$ and vary the number of vertices in the Cube dataset. Indeed, we find that the behavior of the worst-case bounds suggests an unfavorable scaling in the problem dimension: at $s^3 = 8$ vertices, the worst-case bound overestimates the true error by approximately an order of magnitude; at $s^3 = 1000$, it overestimates the true error by approximately 3 orders of magnitude. It is unclear, at present, whether it is possible to remove this dependence on the problem dimension, or whether there are particular configurations of \tilde{Q} and Q of the structure encountered in rotation averaging and pose-graph SLAM that produce estimates attaining the bounds. A more sophisticated analysis considering the specific structure of these matrices may yield more refined bounds.

6.2 Evaluation on standard SLAM benchmark datasets

In these experiments, we consider evaluation of the spectral initialization method on several standard SLAM benchmark datasets. Figure 3 provides a qualitative comparison of three techniques for initialization: odometry only (i.e. composing measurements between consecutive poses), the proposed spectral initialization approach, and the globally optimal solution. We observe that spectral initialization provides solutions that visually resemble the globally optimal solution. Table 1 gives our quantitative results. For each method, we provide the computation time, objective value, and number of iterations required for a Riemannian trust-region (RTR) optimization method to converge to the globally optimal solution. With the exception of odometry-only initialization, all of the methods considered enabled the recovery of (verifiably) globally optimal solutions using SE-Sync: in these cases, initialization methods coupled with standard optimization techniques recovered globally optimal solutions *without* the need to explicitly solve a large-scale semidefinite program.

Both of the spectral methods (using the “full” pose-graph optimization data matrix \tilde{Q} and the

Dataset		Odometry	Chordal	Spectral (Rotation Only)	Spectral	Global Opt.
Sphere	Iter	65	6	8	4	
	Cost	1.14×10^9	1971.17	5594.19	1742.75	1687
	Time (s)	-	0.707	0.602	0.779	
Torus	Iter	32	5	5	4	
	Cost	3.87×10^8	24669.2	25833.2	24272.7	24227
	Time (s)	-	1.316	1.501	1.199	
Grid	Iter	30	6	6	4	
	Cost	1.97×10^{10}	87252	86966.1	84486.4	84320
	Time (s)	-	8.747	18.806	0.25	
Garage	Iter	1028	3	4	4	
	Cost	2.31×10^9	1.42	3.215	2.7	1.26
	Time (s)	-	0.201	0.136	25.7	

Table 1: **Standard SLAM benchmarks** Objective value (cost), time, and number of RTR iterations (Iter.) required to compute SLAM solutions for several standard benchmarks. Proposed approaches are **bold**.

“rotation only” version using only $L(\tilde{G}^\rho)$) provide estimates competitive with the state-of-the-art chordal initialization method, generally attaining near-optimal objective values.⁶ Interestingly, in their work, Moreira et al. [21] found that the rotation-only spectral estimator attains a higher cost on the Sphere dataset than alternative methods, as we do here; however, when we include the translation measurements, we find that this discrepancy disappears. Similarly, the chordal estimator also performs well on this dataset, despite the fact that, like the rotation-only spectral initialization, it does not make use of translation information.

7 Conclusion

In this work, we presented the first performance guarantees for an initialization method in the context of robot perception problems (i.e. assuming incomplete graphs and typical noise models). In particular, the spectral relaxation of the original rotation averaging (resp. pose-graph SLAM) problem admits a solution in terms of the eigenvectors of the data matrix parameterizing the problem which has error upper-bounded as a function of the noise corrupting the data. These bounds also allow us to reason about the worst-case deviation of an initial guess from a maximum-likelihood estimate. Finally, we empirically examine the tightness of these bounds and compare the quality of two different spectral initializers in the context of 3D pose-graph SLAM applications using benchmark datasets.

The bounds presented here also emphasize an important connection between the spectral graph-theoretic properties of the graph parameterizing rotation averaging and SLAM problems and the error of estimators for those problems. This arises through the presence of the value $\lambda_{d+1}(Q)$, the algebraic connectivity of the rotation weight Laplacian in the case of rotation averaging, in the error bounds.

Moreover, the use of initialization techniques with performance guarantees raises an interesting line of reasoning. By virtue of the nonconvexity of Problem 3, the maximum-likelihood estimator attaining the performance bound in Theorem 5 may be difficult to obtain and indeed

⁶Our current implementation is aimed at recovering high-precision eigenvector estimates, rather than expedient computation. Despite this, spectral initialization is often faster than the chordal approach, though occasionally this added precision leads to longer computation times than would be necessary to obtain a good estimate, e.g. on the Garage dataset.

may be impossible to *verify*. Rosen et al. [24] observed problems in the high-noise regime where verification of solutions to the maximum-likelihood estimation problem for pose-graph SLAM could not be verified, but nonetheless where descent methods coupled with chordal initialization could obtain reasonable solutions. In contrast, for these problems the spectral estimator, which attains a similar worst-case error bound, can *always* be computed (and indeed may provide a very reasonable starting point for subsequent refinement using a descent method).

Finally, in practice one does not have access to the error matrix ΔQ . In practical applications where we would like to understand the performance of estimators for these problems *a priori* (i.e. given only the noise statistics of a set of sensors and the topology of the graph), we may resort practically to empirical statistics about $\|\Delta Q\|_2$ by simulation of noisy measurements using the generative model.

A Symmetric perturbations of symmetric matrices

Recall that \underline{R} and Φ are the solutions of the noiseless and noisy versions of the spectral relaxation in Problem 4. It is straightforward to verify that these are in fact Stiefel manifold elements giving the d minimum eigenvectors for their corresponding data matrices. The Davis-Kahan Theorem is a classical result in linear algebra that measures the perturbation of a matrix's eigenvectors under a symmetric perturbation of that matrix [27]. Therefore, we make use of this theorem to derive a bound on the estimation error of a spectral estimator as a function of the noise in the data matrix. In particular, the proof of Lemma 2 (and consequently Theorem 4) relies on a particular variant of the Davis-Kahan $\sin \theta$ Theorem [30, Theorem 2]. Here, we briefly restate the main result of [30] and give a proof of Lemma 2.

Theorem 7 (Yu et al. [30], Theorem 2). *Let $\Sigma, \hat{\Sigma} \in \mathbb{R}^{p \times p}$ be symmetric, with eigenvalues $\lambda_1 \leq \dots \leq \lambda_p$ and $\hat{\lambda}_1 \leq \dots \leq \hat{\lambda}_p$ respectively. Fix $1 \leq r \leq s \leq p$ and assume that $\min(\lambda_r - \lambda_{r-1}, \lambda_{s+1} - \lambda_s) > 0$, where $\lambda_0 \triangleq -\infty$ and $\lambda_{p+1} \triangleq \infty$. Let $d \triangleq s - r + 1$, and let $V = (v_r, v_{r+1}, \dots, v_s) \in \mathbb{R}^{p \times d}$ and $\hat{V} = (\hat{v}_r, \hat{v}_{r+1}, \dots, \hat{v}_s) \in \mathbb{R}^{p \times d}$ have orthonormal columns satisfying $\Sigma v_j = \lambda_j v_j$ and $\hat{\Sigma} \hat{v}_j = \hat{\lambda}_j \hat{v}_j$ for $j = r, r+1, \dots, s$. Then there exists an orthogonal matrix $G \in O(d)$ such that*

$$\|\hat{V}G - V\|_F \leq \frac{2^{3/2} \min(d^{1/2} \|\hat{\Sigma} - \Sigma\|_{op}, \|\hat{\Sigma} - \Sigma\|_F)}{\min(\lambda_r - \lambda_{r-1}, \lambda_{s+1} - \lambda_s)}. \quad (31)$$

With this result in hand, we are ready to prove Lemma 2.

Proof of Lemma 2. The data matrices \tilde{Q} and \underline{Q} are symmetric $dn \times dn$ matrices with eigenvalues $\lambda_1 \leq \dots \leq \lambda_{dn}$ and $\tilde{\lambda}_1 \leq \dots \leq \tilde{\lambda}_{dn}$, respectively. It is straightforward to verify from the statement of Problem 4 that the d normalized eigenvectors corresponding to $\lambda_1, \dots, \lambda_d$ of \underline{Q} and $\tilde{\lambda}_1, \dots, \tilde{\lambda}_d$ are exactly $\frac{1}{\sqrt{n}} R^\top$ and $\frac{1}{\sqrt{n}} \Phi^\top$, respectively. Then, letting $s = 1$ and $r = d$ and applying Theorem 7, there exists an orthogonal matrix $G \in O(d)$ such that:

$$\frac{1}{\sqrt{n}} \|\Phi^\top G - \underline{R}^\top\|_F \leq \frac{2\sqrt{2d} \|\tilde{Q} - \underline{Q}\|_2}{\lambda_{d+1}(\underline{Q}) - \lambda_d(\underline{Q})}. \quad (32)$$

Multiplying both sides of this expression by \sqrt{n} , we have:

$$\|\Phi^\top G - \underline{R}^\top\|_F \leq \frac{2\sqrt{2dn} \|\tilde{Q} - \underline{Q}\|_2}{\lambda_{d+1}(\underline{Q}) - \lambda_d(\underline{Q})}. \quad (33)$$

Now, by definition $\Delta Q = \tilde{Q} - Q$, and from the fact that $\underline{R}^\top \in \ker(Q)$ and that $\lambda_{d+1}(Q) > 0$ (since \mathcal{G} is connected),⁷ we have that $\lambda_d = 0$ and the above expression simplifies to:

$$\|\Phi^\top G - \underline{R}^\top\|_F \leq \frac{2\sqrt{2dn}\|\Delta Q\|_2}{\lambda_{d+1}(Q)}. \quad (34)$$

Taking the transpose of the terms inside the norm gives the desired result. \square

B Proof of the main results

In this section, we prove the main results, i.e. Theorem 4, Theorem 5, and Corollary 6.

B.1 An upper bound for the estimation error in Problem 4

Proof. To simplify the subsequent derivation, we will assume without loss of generality that \underline{R} and Φ are the representatives of their orbits satisfying $d_{\mathcal{O}}(\underline{R}, \Phi) = \|\underline{R} - \Phi\|_F$. Recall from the definition of $d_{\mathcal{S}}(\underline{R}, \underline{R}^{(0)})$ that:

$$d_{\mathcal{S}}(\underline{R}, \underline{R}^{(0)}) = \min_{G \in \mathrm{SO}(d)} \|\underline{R} - GR^{(0)}\|_F. \quad (35)$$

Therefore, we have:

$$\begin{aligned} d_{\mathcal{S}}(\underline{R}, \underline{R}^{(0)})^2 &= \min_{G \in \mathrm{SO}(d)} \|\underline{R} - GR^{(0)}\|_F^2 \\ &\leq \|\underline{R} - R^{(0)}\|_F^2, \\ &= \sum_{i=1}^n \|R_i - \Pi_{\mathcal{S}}(\Phi_i)\|_F^2, \end{aligned} \quad (36)$$

where in the last line we have used the fact that $R^{(0)}$ consists of the projections of individual $(d \times d)$ blocks of Φ onto $\mathrm{SO}(d)$. From Lemma 3, we have that each of the n summands above satisfies:

$$\|R_i - \Pi_{\mathcal{S}}(\Phi_i)\|_F^2 \leq 4\|R_i - \Phi_i\|_F^2. \quad (37)$$

This, in turn, gives a corresponding bound on the summation:

$$\begin{aligned} \sum_{i=1}^n \|R_i - \Pi_{\mathcal{S}}(\Phi_i)\|_F^2 &\leq 4 \sum_{i=1}^n \|R_i - \Phi_i\|_F^2 \\ &= 4\|\underline{R} - \Phi\|_F^2. \end{aligned} \quad (38)$$

Since, by hypothesis, Φ and \underline{R} are representatives of their orbits satisfying $d_{\mathcal{O}}(\underline{R}, \Phi) = \|\underline{R} - \Phi\|_F$, we have:

$$4\|\underline{R} - \Phi\|_F^2 = 4d_{\mathcal{O}}(\underline{R}, \Phi)^2. \quad (39)$$

Applying Lemma 2, we directly obtain:

$$4d_{\mathcal{O}}(\underline{R}, \Phi)^2 \leq 4(2\sqrt{2dn})^2 \frac{\|\Delta Q\|_2^2}{\lambda_{d+1}(Q)^2}. \quad (40)$$

⁷It is not particularly restrictive to assume that \mathcal{G} is connected. In the case that \mathcal{G} is not connected, the estimation problem splits over the connected components of \mathcal{G} , and all of our results hold separately for each connected component.

In summary, we have:

$$d_S(\underline{R}, \underline{R}^{(0)})^2 \leq 4(2\sqrt{2dn})^2 \frac{\|\Delta Q\|_2^2}{\lambda_{d+1}(Q)^2}. \quad (41)$$

Taking the square root of both sides of the inequality in the last line gives:

$$d_S(\underline{R}, \underline{R}^{(0)}) \leq \frac{4\sqrt{2dn}\|\Delta Q\|_2}{\lambda_{d+1}(Q)}, \quad (42)$$

which concludes the proof. \square

B.2 An upper bound for the estimation error in Problem 3

We begin following the arguments of Prescott [22, Appendix D.4]. From the optimality of R^* we have:

$$\begin{aligned} \text{tr}(\tilde{Q}\underline{R}^\top \underline{R}) &= \text{tr}(\underline{Q}\underline{R}^\top \underline{R}) + \text{tr}(\Delta Q \underline{R}^\top \underline{R}) \\ &\geq \text{tr}(\underline{Q}\underline{R}^{*\top} \underline{R}^*) + \text{tr}(\Delta Q \underline{R}^{*\top} \underline{R}^*) = \text{tr}(\tilde{Q}\underline{R}^{*\top} \underline{R}^*). \end{aligned} \quad (43)$$

Since $\text{tr}(\underline{Q}\underline{R}^\top \underline{R}) = 0$, we can rearrange the above expression to obtain:

$$\text{tr}(\underline{Q}\underline{R}^{*\top} \underline{R}^*) \leq \text{tr}(\Delta Q \underline{R}^\top \underline{R}) - \text{tr}(\Delta Q \underline{R}^{*\top} \underline{R}^*). \quad (44)$$

Using the fact that $\text{tr}(\Delta Q \underline{R}^\top \underline{R}) = \text{vec}(\underline{R})^\top (\Delta Q \otimes I_n) \text{vec}(\underline{R})$ (and likewise for $\text{tr}(\Delta Q \underline{R}^{*\top} \underline{R}^*)$), we have:

$$\begin{aligned} \text{tr}(\underline{Q}\underline{R}^{*\top} \underline{R}^*) &\leq \text{vec}(\underline{R} - \underline{R}^*)^\top (\Delta Q \otimes I_n) \text{vec}(\underline{R} + \underline{R}^*) \\ &\leq \|\text{vec}(\underline{R} - \underline{R}^*)\|_2 \|\Delta Q \otimes I_n\|_2 \|\text{vec}(\underline{R} + \underline{R}^*)\|_2 \\ &= \|\underline{R} - \underline{R}^*\|_F \|\Delta Q\|_2 \|\underline{R} + \underline{R}^*\|_F \\ &\leq 2\sqrt{dn} \|\underline{R} - \underline{R}^*\|_F \|\Delta Q\|_2. \end{aligned} \quad (45)$$

In order to lower-bound the right-hand side of (45) in terms of the estimation error $d_S(\underline{R}, \underline{R}^*)$, we will make use of the following technical lemma of Rosen et al. [24]:

Lemma 8 (Lemma 11 of Rosen et al. [24]). *Let $\underline{R} \in \mathcal{O}(d)^n \subset \mathbb{R}^{d \times dn}$ and furthermore let $M = \{W\underline{R} \mid W \in \mathbb{R}^{d \times d}\} \subset \mathbb{R}^{d \times dn}$ be the subspace of matrices with rows contained in $\text{image}(\underline{R}^\top)$. Then*

$$\begin{aligned} \text{Proj}_V : \mathbb{R}^{dn} &\rightarrow \text{image}(\underline{R}^\top) \\ \text{Proj}_V(x) &= \frac{1}{n} \underline{R}^\top \underline{R} x \end{aligned} \quad (46)$$

is the orthogonal projection onto $\text{image}(\underline{R}^\top)$ with respect to the ℓ_2 inner product, and the map

$$\begin{aligned} \text{Proj}_M : \mathbb{R}^{d \times dn} &\rightarrow M \\ \text{Proj}_M(X) &= \frac{1}{n} X \underline{R}^\top \underline{R} \end{aligned} \quad (47)$$

which applies Proj_V to the rows of X is the orthogonal projection onto M with respect to the Frobenius inner product.

Since $\ker(Q) = \text{image}(\underline{R}^\top)$ and $\dim(\text{image}(\underline{R}^\top)) = d$, from Lemma 8, we have:

$$\text{tr}(\underline{Q}\underline{R}^{*\top} \underline{R}^*) \geq \lambda_{d+1}(Q) \|P\|_F^2, \quad (48)$$

where

$$\begin{aligned} R^* &= K + P \\ K &= \text{Proj}_M(R^*) = \frac{1}{n} R^* \underline{R}^\top \underline{R} \\ P &= R^* - \text{Proj}_M(R^*) = R^* - \frac{1}{n} R^* \underline{R}^\top \underline{R} \end{aligned} \tag{49}$$

is an orthogonal decomposition of R^* and the rows of P are contained in the orthogonal complement of $\text{image}(\underline{R}^\top)$

The following lemma provides a bound on $d_S(R, R^*)^2$ in terms of $\|P\|_F^2$.

Lemma 9. *Let R^* and \underline{R} be representatives of their orbits such that $d_S(R, R^*) = \|\underline{R} - R^*\|_F$, and $P = R^* - \text{Proj}_M(R^*)$ as defined in (49). Then:*

$$\frac{1}{4} d_S(R, R^*)^2 \leq \|P\|_F^2. \tag{50}$$

Proof. Let $X = \frac{1}{n} \underline{R} R^{*\top}$, so that $K = X^\top \underline{R}$. Expanding the left hand side, we have:

$$\begin{aligned} d_S(R, R^*)^2 &= \|R^* - \underline{R}\|_F^2 \\ &\leq \|R^* - \Pi_S(X^\top) \underline{R}\|_F^2, \end{aligned} \tag{51}$$

from the fact that the orbit distance is obtained as the minimum over $G \in \text{SO}(d)$ of the quantity $\|R^* - G \underline{R}\|_F$, and that by hypothesis this minimum is obtained as $\|R^* - \underline{R}\|_F$. Breaking up the norm into its blockwise summands, and from the orthogonal invariance of the Frobenius norm, we can rearrange this expression as follows:

$$\begin{aligned} \|R^* - \Pi_S(X^\top) \underline{R}\|_F^2 &= \sum_{i=1}^n \|R_i^* - \Pi_S(X^\top) R_i\|_F^2 \\ &= \sum_{i=1}^n \|R_i^* \underline{R}_i^\top - \Pi_S(X^\top)\|_F^2. \end{aligned} \tag{52}$$

From Lemma 3, we know that each summand in the above expression satisfies

$$\|R_i^* \underline{R}_i^\top - \Pi_S(X^\top)\|_F^2 \leq 4 \|R_i^* \underline{R}_i^\top - X^\top\|_F^2. \tag{53}$$

Since this bound is satisfied for each summand, the total summation satisfies

$$\begin{aligned} \sum_{i=1}^n \|R_i^* \underline{R}_i^\top - \Pi_S(X^\top)\|_F^2 &\leq 4 \sum_{i=1}^n \|R_i^* \underline{R}_i^\top - X^\top\|_F^2 \\ &= 4 \sum_{i=1}^n \|R_i^* - X^\top \underline{R}_i\|_F^2 \\ &= 4 \|R^* - X^\top \underline{R}\|_F^2. \end{aligned} \tag{54}$$

Since $K = X^\top \underline{R}$, we have:

$$\begin{aligned} 4 \|R^* - X^\top \underline{R}\|_F^2 &= 4 \|R^* - K\|_F^2 \\ &= 4 \|P\|_F^2, \end{aligned} \tag{55}$$

which gives the desired bound. \square

With this result, we are ready to prove Theorem 5.

Proof. From (48) and (45), we have:

$$\lambda_{d+1}(\underline{Q})\|P\|_F^2 \leq 2\sqrt{dn}\|\underline{R} - R^*\|_F\|\Delta Q\|_2. \quad (56)$$

Since, by hypothesis, R^* and \underline{R} are the representatives of their orbits satisfying $d_S(\underline{R}, R^*) = \|\underline{R} - R^*\|_F$, from Lemma 9 we have

$$d_S(\underline{R}, R^*)^2 \leq 4\|P\|_F^2. \quad (57)$$

Combining (57) with (56), we obtain:

$$d_S(\underline{R}, R^*) \leq \frac{8\sqrt{dn}\|\Delta Q\|_2}{\lambda_{d+1}(\underline{Q})}, \quad (58)$$

which is what we intended to show. \square

B.3 An upper bound on the distance between a spectral estimator and the maximum-likelihood estimator

Lemma 10 (Orbit distances are pseudometrics). *The orbit distances d_S and d_O are pseudometrics on $\text{SO}(d)^n$ and $\text{O}(d)^n$, respectively. In particular, for all $X, Y, Z \in \text{SO}(d)^n$, we have:*

1. $d_S(X, X) = 0$
2. $d_S(X, Y) = d_S(Y, X)$
3. $d_S(X, Z) \leq d_S(X, Y) + d_S(Y, Z)$,

and likewise for d_O .

Proof. To simplify the subsequent derivation, we will continue with the proof for the case of d_S on $\text{SO}(d)^n$, but the same methodology applies directly to d_O on $\text{O}(d)^n$. A *pseudometric* on $\text{SO}(d)^n$ (resp. $\text{O}(d)^n$) is any nonnegative function $\text{SO}(d)^n \times \text{SO}(d)^n \rightarrow \mathbb{R}_{\geq 0}$ satisfying the properties 1–3 [16]. To establish 1, we have:

$$d_S(X, X) = \min_{G \in \text{SO}(d)} \|X - GX\|_F = 0, \quad (59)$$

since $\|A\|_F \geq 0$ for all A and taking $G = I$ realizes this minimum value.

For 2, we have:

$$\begin{aligned} d_S(X, Y) &= \min_{G \in \text{SO}(d)} \|X - GY\|_F \\ &= \min_{G \in \text{SO}(d)} \|Y - G^\top X\|_F = d_S(Y, X), \end{aligned} \quad (60)$$

where the second line follows from the orthogonal invariance of the Frobenius norm, and the last line follows from the fact that since $G^\top = G^{-1} \in \text{SO}(d)$, then G^\top ranges over all of $\text{SO}(d)$ as G does.

Finally, to establish 3, we aim to prove that for any $X, Y, Z \in \text{SO}(d)^n$:

$$d_S(X, Z) \leq d_S(X, Y) + d_S(Y, Z). \quad (61)$$

Suppose the orbit distance $d_S(X, Y)$ is attained with minimizer $G_{XY}^* \in \text{SO}(d)$ and likewise the distance $d_S(Y, Z)$ is attained with minimizer $G_{YZ}^* \in \text{SO}(d)$. Define:

$$G' \triangleq G_{XY}^* G_{YZ}^*. \quad (62)$$

Now, since G' is itself the product of two elements of $\text{SO}(d)$, we know $G' \in \text{SO}(d)$, and therefore:

$$d_{\mathcal{S}}(X, Z) = \min_{G \in \text{SO}(d)} \|X - GZ\|_F \leq \|X - G'Z\|_F. \quad (63)$$

Examining the right-hand side of this expression, we have:

$$\begin{aligned} \|X - G'Z\|_F &= \|X - G_{XY}^*Y + G_{XY}^*Y - G'Z\|_F \\ &\leq \underbrace{\|X - G_{XY}^*Y\|_F}_{d_{\mathcal{S}}(X, Y)} + \|G_{XY}^*Y - G'Z\|_F, \end{aligned} \quad (64)$$

where the last line follows from the triangle inequality for the Frobenius norm. Now, substitution of the definition (62) into the second term of (64) reveals:

$$\begin{aligned} \|G_{XY}^*Y - G'Z\|_F &= \|G_{XY}^*Y - G_{XY}^*G_{YZ}^*Z\|_F \\ &= \|Y - G_{YZ}^*Z\|_F \\ &= d_{\mathcal{S}}(Y, Z), \end{aligned} \quad (65)$$

where the second line follows from the orthogonal invariance of the Frobenius norm. Taken together, these results give:

$$d_{\mathcal{S}}(X, Z) \leq \|X - G'Z\|_F \leq d_{\mathcal{S}}(X, Y) + d_{\mathcal{S}}(Y, Z), \quad (66)$$

which is what we intended to show. \square

Lemma 10 suggests a straightforward proof of Corollary 6.

Proof. From the triangle inequality for $d_{\mathcal{S}}$, we have:

$$d_{\mathcal{S}}(R^{(0)}, R^*) \leq d_{\mathcal{S}}(\underline{R}, R^{(0)}) + d_{\mathcal{S}}(\underline{R}, R^*). \quad (67)$$

Substitution of (26) and (27) into (67) gives the desired result. \square

C Relationship to the method of Moreira et al. [21]

In their recent work, Moreira et al. [21] construct an estimator for pose-graph SLAM problems based on eigenvector computations (and a computationally-efficient procedure for eigenvector recovery). In this section, we show that their approach is formally equivalent to the *rotation-only* variant of the spectral initialization we discuss in Section 5 and therefore has estimation error satisfying the bound (30). Moreira et al. [21] specifically consider *unweighted* rotation measurements, for which it suffices to consider the generative model (6) taking $\kappa_{ij} = 1$ for all edges $(i, j) \in \mathcal{E}$.

Their construction begins by considering the matrix $\tilde{M} \in \mathbb{R}^{dn \times dn}$ with $d \times d$ block i, j given by:

$$\tilde{M}_{ij} = \begin{cases} \tilde{R}_{ij} & \text{if } (i, j) \in \mathcal{E} \\ I_d & \text{if } i = j \\ 0_d & \text{otherwise.} \end{cases} \quad (68)$$

They observe that for all stationary points $\hat{R} \in \text{SO}(d)^n \subset \mathbb{R}^{d \times dn}$, there is a corresponding matrix $\Lambda \in \mathbb{R}^{dn \times dn}$ such that:

$$\underbrace{(\Lambda - \tilde{M})}_{S} \hat{R}^\top = 0, \quad (69)$$

where Λ has the symmetric $d \times d$ block diagonal structure:

$$\Lambda = \begin{bmatrix} \Lambda_1 & \cdots & 0 \\ \vdots & \ddots & \vdots \\ 0 & \cdots & \Lambda_n \end{bmatrix}. \quad (70)$$

In the *noiseless* case where $\tilde{M} = \underline{M}$,⁸ the matrix $S = \Lambda - \underline{M}$ is given by (cf. [21, Equation 14]):

$$S = (\mathcal{L} \otimes J_d) \circ \underline{M}, \quad (71)$$

where \mathcal{L} is the scalar (unweighted) rotation graph Laplacian, $J_d \in \mathbb{R}^{d \times d}$ is an all-ones matrix, and \circ denotes the Hadamard product. That is, \mathcal{L} is equivalent to $L(W^\rho)$ where $\kappa_{ij} = 1$ for all $(i, j) \in \mathcal{E}$. It is straightforward to verify from the definition in (13a) that $S = L(G^\rho)$. It follows that $S \succeq 0$ and $\underline{R}^\top \in \ker(S)$, so the ground-truth rotations \underline{R} can be recovered by computing the d eigenvectors of S corresponding to the smallest eigenvalues of S . In the case of noisy measurements, Moreira et al. [21] compute the eigenvectors of $S = (\mathcal{L} \otimes J_3) \circ \tilde{M}$. Once again, by comparing the definition, we observe that the quantity $(\mathcal{L} \otimes J_3) \circ \tilde{M}$ is identical to $L(\tilde{G}^\rho)$ (cf. equation (13a)) constructed from the noisy measurements, and with $\kappa_{ij} = 1$. Consequently, their spectral estimator based on recovering eigenvectors of S is identical to the procedure outlined in Section 4 in the case of unweighted measurements, and where translation measurements have been discarded (i.e. the rotation-only case discussed in Section 5).

References

- [1] Federica Arrigoni, Beatrice Rossi, and Andrea Fusiello. Spectral synchronization of multiple views in $\text{SE}(3)$. *SIAM Journal on Imaging Sciences*, 9(4):1963–1990, 2016.
- [2] Afonso S Bandeira, Nicolas Boumal, and Amit Singer. Tightness of the maximum likelihood semidefinite relaxation for angular synchronization. *Mathematical Programming*, 163(1-2):145–167, 2017.
- [3] Byron Boots and Geoff Gordon. A spectral learning approach to range-only SLAM. In *International Conference on Machine Learning*, pages 19–26. PMLR, 2013.
- [4] Nicolas Boumal. Nonconvex phase synchronization. *SIAM Journal on Optimization*, 26(4):2355–2377, 2016.
- [5] Nicolas Boumal, Amit Singer, and P-A Absil. Robust estimation of rotations from relative measurements by maximum likelihood. In *52nd IEEE Conference on Decision and Control*, pages 1156–1161. IEEE, 2013.
- [6] Nicolas Boumal, Amit Singer, P-A Absil, and Vincent D Blondel. Cramér–Rao bounds for synchronization of rotations. *Information and Inference: A Journal of the IMA*, 3(1):1–39, 2014.
- [7] Jesus Briales and Javier Gonzalez-Jimenez. Cartan-Sync: Fast and global $\text{SE}(d)$ -synchronization. *IEEE Robotics and Automation Letters*, 2(4):2127–2134, 2017.

⁸In keeping with the notation in the rest of this manuscript, we use the notation \underline{M} to denote the measurement matrix (68) constructed from the *ground-truth* rotations R_{ij} .

- [8] Luca Carlone, David M Rosen, Giuseppe Calafiore, John J Leonard, and Frank Dellaert. Lagrangian duality in 3D SLAM: Verification techniques and optimal solutions. In *2015 IEEE/RSJ International Conference on Intelligent Robots and Systems (IROS)*, pages 125–132. IEEE, 2015.
- [9] Luca Carlone, Roberto Tron, Kostas Daniilidis, and Frank Dellaert. Initialization techniques for 3D SLAM: a survey on rotation estimation and its use in pose graph optimization. In *2015 IEEE International Conference on Robotics and Automation (ICRA)*, pages 4597–4604. IEEE, 2015.
- [10] Luca Carlone, Giuseppe C Calafiore, Carlo Tommolillo, and Frank Dellaert. Planar pose graph optimization: Duality, optimal solutions, and verification. *IEEE Transactions on Robotics*, 32(3):545–565, 2016.
- [11] Yongbo Chen, Shoudong Huang, Liang Zhao, and Gamini Dissanayake. Cramér–Rao bounds and optimal design metrics for pose-graph SLAM. *IEEE Transactions on Robotics*, 37(2):627–641, 2021.
- [12] Frank Dellaert, David M Rosen, Jing Wu, Robert Mahony, and Luca Carlone. Shonan rotation averaging: Global optimality by surfing $\text{SO}(p)^N$. In *European Conference on Computer Vision*, pages 292–308. Springer, 2020.
- [13] Taosha Fan, Hanlin Wang, Michael Rubenstein, and Todd Murphy. CPL-SLAM: Efficient and certifiably correct planar graph-based SLAM using the complex number representation. *IEEE Transactions on Robotics*, 36(6):1719–1737, 2020.
- [14] Giorgio Grisetti, Rainer Kummerle, Cyrill Stachniss, and Wolfram Burgard. A tutorial on graph-based SLAM. *IEEE Intelligent Transportation Systems Magazine*, 2(4):31–43, 2010.
- [15] Richard J Hanson and Michael J Norris. Analysis of measurements based on the singular value decomposition. *SIAM Journal on Scientific and Statistical Computing*, 2(3):363–373, 1981.
- [16] John L Kelley. *General Topology*. Van Nostrand, New York, 1955.
- [17] Kasra Khosoussi, Shoudong Huang, and Gamini Dissanayake. Novel insights into the impact of graph structure on SLAM. In *2014 IEEE/RSJ International Conference on Intelligent Robots and Systems*, pages 2707–2714. IEEE, 2014.
- [18] Shuyang Ling. Near-optimal performance bounds for orthogonal and permutation group synchronization via spectral methods. *arXiv preprint arXiv:2008.05341*, 2020.
- [19] Huikang Liu, Man-Chung Yue, and Anthony Man-Cho So. A unified approach to synchronization problems over subgroups of the orthogonal group. *arXiv preprint arXiv:2009.07514*, 2020.
- [20] Daniel Martinec and Tomas Pajdla. Robust rotation and translation estimation in multiview reconstruction. In *2007 IEEE Conference on Computer Vision and Pattern Recognition*, pages 1–8. IEEE, 2007.
- [21] Gabriel Moreira, Manuel Marques, and Joao Paulo Costeira. Fast Pose Graph Optimization via Krylov–Schur and Cholesky Factorization. In *Proceedings of the IEEE/CVF Winter Conference on Applications of Computer Vision*, pages 1898–1906, 2021.

- [22] Brian Patrick Preskitt. *Phase retrieval from locally supported measurements*. PhD thesis, UC San Diego, 2018.
- [23] Yixuan Qiu. Spectra: C++ library for large scale eigenvalue problems. <https://spectralib.org>, 2015.
- [24] David M Rosen, Luca Carlone, Afonso S Bandeira, and John J Leonard. SE-Sync: A certifiably correct algorithm for synchronization over the special Euclidean group. *The International Journal of Robotics Research*, 38(2-3):95–125, 2019.
- [25] David M Rosen, Kevin J Doherty, Antonio Terán Espinoza, and John J Leonard. Advances in Inference and Representation for Simultaneous Localization and Mapping. *Annual Review of Control, Robotics, and Autonomous Systems*, 4, 2021.
- [26] Amit Singer. Angular synchronization by eigenvectors and semidefinite programming. *Applied and computational harmonic analysis*, 30(1):20–36, 2011.
- [27] G.W. Stewart, J.W. Stewart, J. Sun, Academic Press (Londyn)., and Harcourt Brace Johnson. *Matrix Perturbation Theory*. Computer Science and Scientific Computing. Elsevier Science, 1990. ISBN 9780126702309. URL <https://books.google.com/books?id=178PAQAAQAAJ>.
- [28] Yulun Tian, Kasra Khosoussi, David M Rosen, and Jonathan P How. Distributed certifiably correct pose-graph optimization. *arXiv preprint arXiv:1911.03721*, 2019.
- [29] Shinji Umeyama. Least-squares estimation of transformation parameters between two point patterns. *IEEE Transactions on Pattern Analysis & Machine Intelligence*, 13(04):376–380, 1991.
- [30] Yi Yu, Tengyao Wang, and Richard J Samworth. A useful variant of the Davis–Kahan theorem for statisticians. *Biometrika*, 102(2):315–323, 2015.